Chapter 5

Experiment 2: Drag of Simple Shapes and Calibration of Force Balance

5.1 Objective

The objective of this experiment is to determine the drag and drag coefficient on blunt and streamlined objects as a function of velocity and boundary layer type, i.e., laminar or turbulent.

5.2 Overview

Total drag on objects in high Reynolds number and incompressible flows consists of skin friction and pressure drag. Viscous forces at the surface of the object results in skin friction drag. At moderate Reynolds numbers, pressure drag dominates the total drag. For example, a sphere at a Reynolds number of 1000 has a skin friction drag approximately equal to 5% of the pressure drag. However, on streamlined objects, the skin friction drag can become a large fraction of the total drag. An unequal pressure distribution on the upstream- and downstream-facing surfaces of the object results in pressure drag. The unequal pressure distribution arises because of separation of the boundary layer. The point at which separation occurs, and hence the magnitude of the pressure drag, depends on the shape of the object and whether the boundary layer is laminar or turbulent. The chapter will discuss the effect of shape on drag and the instrumentation used to measure the drag force.

5.2.1 Effect of Shape on Drag

The shape of the object has a significant effect on the drag as it determines the pressure gradient in the fluid. Starting at the upstream stagnation point and extending to about the point of maximum thickness, the pressure gradient is said to be favorable, i.e., the pressure decreases and the velocity in the freestream increases with increasing downstream position. In this region, the net pressure force acts in the downstream direction and aids the flow?s motion. Near the point of maximum thickness, the pressure reaches a minimum, at which point the pressure begins to increase with increasing downstream position. In this region (downstream of the point of maximum thickness), the pressure gradient is said to be unfavorable as the net pressure force on a fluid particle acts in the direction opposite to the flow. If the unfavorable pressure gradient is large enough, the fluid in the boundary layer, which is also retarded due to viscous effects, can be brought to rest at a point close to but not on the solid surface (at the solid surface, the fluid velocity is always zero to satisfy the no-slip condition). Mathematically, the point at which the fluid velocity near the surface becomes zero is the position where $\frac{\partial u}{\partial y}\big|_{y=0} = 0$ and is defined as the separation point.

Consideration of the equation for conservation of mass and Bernoulli?s equation leads to the conclusion that an object with a faster rate of change of thickness in the downstream direction will have a larger unfavorable pressure gradient than one with a smaller rate of change of thickness in the downstream direction. Thus, a sphere will have a larger retarding pressure force downstream of the point of maximum thickness than that of a streamline - or teardrop - shaped object with the same maximum thickness. The larger retarding pressure forces on the sphere means the flow will more likely separate from the sphere than from the streamlined object. For this reason, the sphere should experience greater pressure drag than the streamlined object. Note, however, the larger surface area of the streamlined object will result in greater skin friction drag than a sphere. Nonetheless, at moderate to high Reynolds numbers pressure drag dominates, meaning the streamlined object will have a lower measured total drag, assuming both objects have the same maximum thickness.

5.2.2 Effect of Boundary Layer Type on Drag

On objects with large, unfavorable pressure gradients, e.g., a sphere, the location of the separation point and the magnitude of the pressure drag depends significantly on whether the fluid in the boundary layer is laminar or turbulent. Turbulent boundary layers contain eddies that increase the transportation of fluid particles of high momentum from the outer portion of the boundary layer to the low momentum portion of the boundary layer near the wall. The increase in momentum close to the solid surface allows the boundary layer

to overcome the adverse pressure gradient longer, pushing the boundary layer separation point downstream. The overall effect of the phenomenon is a reduction in the pressure drag on the object. Laminar boundary layers occur at low Reynolds numbers and transitions to turbulence as the Reynolds number increases. The Reynolds number at which transition of the boundary layer from laminar to turbulent occurs depends on the surface geometry and the turbulence level in the freestream. The transition Reynolds number decreases with increasing surface roughness and freestream turbulence. For example, for smooth spheres in a freestream flow with low turbulence levels, a laminar boundary layer has been found in flows with Reynolds numbers as high as 5×10^5. In contrast, modest but low levels of freestream turbulence have been found to lower the transition Reynolds number to about 2×10^5.

5.2.3 Critical Reynolds Number

The Reynolds number at which transition occurs is called the critical Reynolds number. Consider an infinite cylinder in a cross flow, for example. At Reynolds numbers slightly lower than the critical value, the drag coefficient is about 1.2. At higher Reynolds numbers, the drag coefficient is reduced to about 0.25. Thus, one definition of the critical Reynolds number for an infinite cylinder is that the critical Reynolds number, Re_{cr}, is the Reynolds number that corresponds to a sudden decrease in drag coefficient.

5.2.4 Wall Effects on Drag Measurements

In addition to drag measurements on axisymmetric objects, drag measurements on two-dimensional objects such as airfoils are also important. When the end of the object is a finite distance from the wall, the flow may not be two-dimensional because of flow past the edges of the object in addition to the flow of interest over and under the airfoil. If the three-dimensional object can be extended to the wall, it will behave as a two-dimensional object (the three-dimensional end effects will be eliminated) and, thus, the flow will be two-dimensional. (However, at that point the boundary layer growing on the wall may come into play as it impinges on the solid body.)

5.2.5 Force Measurements in Wind Tunnels

In Chapter 7, Barlow et al. (1999), present a comprehensive description of many of the various types of force balances that used to determine the lift and drag on objects in wind tunnels. Balances are generally classified as either *external* or *internal*. As the names

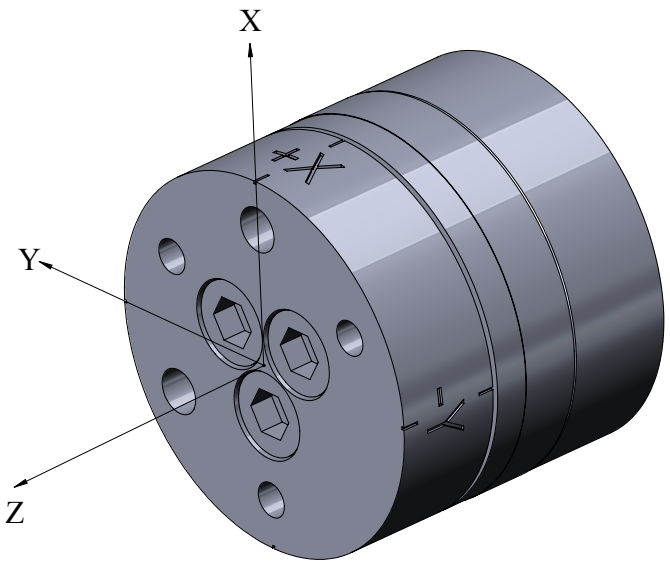

Figure 5.1: ATI Nano 17 force transducer with the measurement axis (ATI-AI, 2017)

suggest, the types are mounted external to the wind tunnel, and the model is connected to the force-measuring sensors by means of struts, wires, or linkages that pass through the tunnel walls. Examples of external balances include the platform, yoke, and pyramidal types. These balances are usually large and fixed relative to the flow direction. The second type of balance is the internal type. Internal force balances are mounted inside the wind tunnel and can be smaller than the model or test object. Internal force balances are typically less expensive and are easier to install. The drawback is that they require more frequent calibration and that their resolution is a function of the maximum force they can withstand. Students will use the ATI NANO17 six-degree of freedom internal force balance shown in figure 5.1. It measures three orthogonal force components, the axial force (F_z) and the two normal forces (F_x and F_y), and three corresponding moments, the roll (T_z), the yaw (T_x) and the pitch (T_y). Note that the positive z axis points upstream, resulting in negative F_z readings during wind tunnel operation.

The ATI NANO17 is based upon a design called a "Maltese cross" shown in figure 5.2. Strain gauges mounted on the three beams form the force transducer. The sensing beams

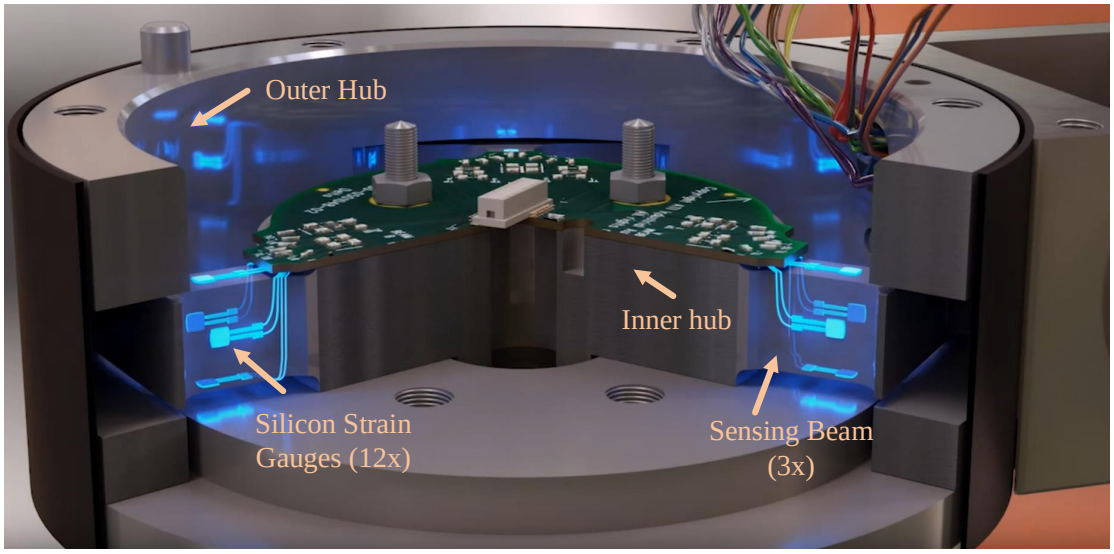

Figure 5.2: Maltese cross design for ATI's Delta force transducer (ATI-AI, 2017)

are machined together with the inner and outer hubs from one blank to form a monolithic structure. This type of construction results in lower hysteresis than designs utilizing beams supported by bolted interfaces. The four strain gauges on each beam (12 total) provide 6 channels of output. Each channel is converted from raw voltage into a strain measurement using a "half bridge" circuit in which one strain gauge is in tension while its companion is in compression (hence twice as many strain gauges as channels; see lecture notes for more details). A precision excitation voltage is supplied from the external ATI power supply module. The strain gauges are oriented on the beams to sense deflection in three orthogonal axes, and the ATI software (resident in the control computer) performs the vector math to convert the sensed voltages into forces and torques. Finally, the results are displayed on the computer monitor using LabView. Even though the NANO17 is a calibrated sensor, the balance will not be capable of making perfect measurements. Three general sources of uncertainty cause the readings to be less than perfect in a strain gauge type sensor. The first arises from misalignment and dimensional variation due to the manufacturing process and assembly. The second is due to interactions of the various components of the force transducers, i.e., the small distortion induced by an axial load in the portion of the force balance designed to be sensitive only to the normal force component. Examples of the third source of uncertainty include the sensitivity of the strain gauges to electronic drift and temperature. Therefore, the sensor calibration should be verified occasionally throughout the course to ensure that it is still providing accurate measurements and to obtain an independent assessment of the calibration accuracy. It is important to note that if the force balance is oriented so that the axis is not parallel to the flow direction, i.e., at some angle of attack,

the axial and normal force vectors will have to be added to give the correct values for the drag and lift forces. (Remember that the drag force is the force component that acts in the direction of the incoming flow, and that the lift force is the force component that acts in a direction normal to the direction of the incoming flow.)

5.3 Experimental Description

5.3.1 Objectives

The goals of the experiment are as follows:

1. Verify the calibration of the force balance and associated electronics.
2. Measure the drag on the large-diameter, smooth sphere at freestream velocities of 5, 10, 15, 20, 25, 30, and 35 m/s. (Be sure to take half of your data in ascending order and half in descending order.)
3. Place a ring made of copper wire on the sphere to serve as a boundary layer trip. The copper ring should be placed such that the stagnation point in the front of the sphere coincides with the center of the copper ring and should have a diameter about 1 cm less than that of the sphere. Measure the drag on the sphere with the ring in place at the same nominal velocities that were used for the smooth sphere.
4. Measure the drag on the streamlined object at the same velocities used for the sphere.
5. Measure the drag on cylinders of various lengths to determine minimum distance from the wall where three-dimensional effects are negligible.

5.3.2 Procedure

The procedure for the various parts of the experiment is as follows:

Calibration of Force Transducer

1. Start with the clear sting in the horizontal position. In the LabView software set offset to zero and gain to 1.
2. Run the LabView program in this configuration. Describe and explain the readings. Should they be all zero? Which one is the largest and why? Due to the Maltese cross design of the transducer, it is not possible to completely get rid of the force in the y-axis, so you will notice a small component on it constantly.

3. Run a measurement and apply the mean of each force and torque reading as the offset, except for T_y. For T_y record the offset value but leave the box at zero on the software. Adjust your spreadsheet software to include this offset value as you go through the experiment. The reason for this is that T_y is the limiting saturation factor in our setup, and we do not want to overwrite the saturation alarm.

4. Run a measurement and verify zero readings.

5. Configure a calibration weight (a maximum total of no more than 400 g), and place it at one set position on the sting.

6. Run a measurement. Record and compare the measured forces and torque to the applied.

7. Move the weight to another set location on the sting and repeat step 6.

8. Repeat steps 5 to 7 for two more weights (typically a light and medium weight work best).

9. Repeat steps 4 through 8 for three more angles of attack, (two positive and one negative) using the same weights and set positions.

10. Plot your results of applied forces and torques vs. the measured forces and torques (from the data acquisition software). The slope of this plot should be within $\pm 5\%$ of 1. **Show the plots to the TA before moving on**.

Drag on a Smooth Sphere

1. Measure the diameter of the sphere and mount the sphere on the force balance. Be sure that the location of the setscrew matches mounting hole on the force-balance. (Be sure to use the small black sphere with a diameter of about 7.5 cm for this experiment.)

2. Set the force balance so that the balance axis is parallel to the flow direction.

3. At zero velocity, set the offset to zero and gain to 1 for the force transducer.

   (a) Run the LabView program in this configuration.

   (b) Place the measured force and torque values in the offset boxes.

   (c) Run the Labview program again to ensure the force and torque readins are approximately zero.

(d) The offset value for the F_z component is $F_{a,0}$ in equation 5.6 and will already be taken into account in the measurement.

4. Install the Pitot-static tube outside of the boundary layer growing on the wall (about 3 *cm* from the wall) of the wind tunnel and connect it to the differential pressure transducer as was done in Experiment 1.

5. Set the velocity to nominal values of 5, 15, 25, 35, 30, 20, 10, and 5 m/s (note the order of the velocities) and record the corresponding values for the axial force from the computer program (you can also write down the values for the other force and moment; do they change appreciably?). Note that test velocity values are acceptable if they are within 5% of the desired values, but be sure to record the measured velocity for each point (If you try to set the velocity exactly, you will waste a lot of time). Record the data in ink on a hard copy of the data sheet and also directly on the data sheet on the computer, plotting the C_D verses Reynolds Number as the data is collected.

6. For each velocity, record the dynamic pressure, $\frac{1}{2}\rho V_\infty^2$, the axial force, F_a, to determine the drag coefficient,

$$C_D \equiv \frac{F_a - F_{a,0}}{\frac{1}{2}\rho V_\infty^2 A_f} \tag{5.1}$$

and the Reynolds number based on the diameter of the sphere. (The density and viscosity should be determined at the laboratory temperature and standard pressure following the procedure in Experiment 1).

7. **Show the drag coefficient as a function of Reynolds number plot to the laboratory assistant.**

Drag on Sphere with Wire Trip

1. After the laboratory assistant has reviewed your plot of drag coefficient as a function of Reynolds number for the smooth sphere, place the copper wire ring on the sphere and secure it with a few pieces of Scotch tape. **Be sure to remove the sphere from the sting balance prior to taping the copper ring in place** (the copper ring should be placed such that the stagnation point on the front of the sphere coincides with the center of the copper ring and should have a diameter about 1 *cm* less than that of the sphere).

2. With the ring in place, repeat all the steps in the procedure for the smooth-sphere measurements.

3. After the assistant has reviewed the plot of the drag coefficient as a function of Reynolds number, carefully remove the sphere from the force balance *then* remove the copper ring from the sphere.

Drag of a Streamlined Object

1. Carefully mount the streamlined object on the force balance.
2. Following the procedure used in the smooth-sphere tests, determine the drag coefficient for the streamlined object as a function of Reynolds number.
3. After the lab assistant has reviewed your plot of the drag coefficient as a function of Reynolds number for the streamlined object, carefully remove the streamlined object from the force balance.

Wall Effects Measurements

1. Record the length of the four different cylinders and measure the width of the wind tunnel test section.
2. Carefully mount one of the cylinders on the force balance by adjusting the screws on the cylinder sides. Use the digital level to ensure a level mount.
3. Using the wall-mounted static taps, set the wind tunnel velocity to approximately 35 m/s, or 10% less than the maximum wind tunnel speed, and record the drag measurement. **Note: The Pitot-static tube cannot be used for this portion of the lab because it will cause the cylinder mounted to the sting balance to oscillate, which may break the force balance!**
4. Turn off the tunnel and carefully remove the cylinder from the sting balance.
5. Repeat steps 2 to 4 for the other cylinders of varying length.

5.3.3 Data Reduction Specific Plots and Tables

1. Create a block diagram and equipment list.
2. On three separate graphs plot the axial force, normal force, and moment as provided by the ATI system as a function of the hand calculated values. Show the calibration equations and lines that correspond to the calibration equations. Be sure to include a legend and a descriptive figure caption.

3. Make a sketch of the test section where the sting balance is aligned with the horizontal direction, and clearly indicate on it the test section floor angle, the free stream angle, both with respect to the sting balance.

4. On one figure with appropriate caption and legend, show the drag coefficient for the smooth sphere, the sphere with copper ring, the streamlined object, and the data for the smooth sphere plotted from a standard fluid mechanics book.

5. Determine the critical Reynolds number for the sphere, tripped sphere, and streamlined boy. Create a table with the values of critical Reynolds numbers.

6. Plot the drag coefficients of the cylinders as a function of the distance of the cylinder from the tunnel wall. On this plot, show the typical cylindrical drag coefficients from a standard textbook.

5.3.4 Specific Questions

1. Which calibration values do you believe are more accurate (ATI output or hand calculations)? Why?

2. What should be the angle of the sting arm for the most accurate measurement of the drag coefficient? Why?

3. Contrast the drag coefficients for the four data sets (sphere, sphere with trip, streamlined object, and longest cylinder) at three Reynolds numbers (minimum, maximum, and a midpoint value) and explain reasons for any differences.

4. Qualitatively comment on the sources of uncertainty in the experimentally measured drag coefficients.

5. Can it be determined from the measured data what the value of the critical Reynolds number is for the smooth sphere or cylinder? How? What are the corresponding theoretical values (refer to your Fluid Mechanics text)?

6. Compare the results of the cylinder drag measurements to standard, two-dimensional textbook values. What is the maximum distance from the wall at which the measured drag coefficient agrees with the standard textbook values? You can identify this distance as the maximum distance of an object from the wall for which the flow can be considered two-dimensional.

Chapter 6

Experiment 3: Drag and Lift for a Clark Y-14 Airfoil with a Leading Edge Slat and a Split Flap

6.1 Objective

In this experiment, students will measure the Lift, Drag, and Pitching Moment of a Clark Y-14 airfoil in a clean configuration, with a slat, with a flap, and with both the slat and the flap. Determination of the pitching moment requires the determination of the location of the aerodynamic center for the clean airfoil. Finally, students will study the influence of changing the flap angle on the aerodynamic properties.

6.2 Overview and Background

6.2.1 Coefficient of Lift, Drag, and Pitching Moment

The lift and drag forces and the pitching moment result from the distribution of viscous and pressure forces on the surface of the airfoil. In the next experiment, students will directly determine the relationship between the lift and drag forces and the pressure and viscous forces. For this experiment, students will use the sting balance to measure the integrated effects of these surface forces and to express those forces in terms of the appropriate non-dimensional coefficients.

The lift force is defined as the component of the force that acts normal to the direction of